PAPER

Development of a self-consistent approximation

IOP Publishing Journal of Physics A: Mathematical and Theoretical
J. Phys. A: Math. Theor. **49** (2016) 095004 (18pp) doi:10.1088/1751-8113/49/9/095004

Development of a self-consistent approximation

V A Ignatchenko and D S Polukhin

L V Kirensky Institute of Physics Siberian Branch of RAS, 660036 Krasnoyarsk, Russia

E-mail: vignatch@iph.krasn.ru

Received 21 April 2015, revised 27 November 2015
Accepted for publication 22 December 2015
Published 25 January 2016

Abstract

A self-consistent approximation of a higher level than the standard self-consistent approximation, known in various fields of physics as the Migdal, Kraichnan or Born self-consistent approximation, is derived taking into account both the first and second terms of the series for the vertex function. In contrast to the standard approximation, the new self-consistent approximation is described by a system of two coupled nonlinear integral equations for the self-energy and the vertex function. In addition to all the diagrams with non-intersecting lines of correlation/interaction taken into account by the standard self-consistent approximation, the new approach takes into account in each term of the Green's function expansion a significant number of diagrams with intersections of these lines. Because of this, the shape, linewidth, and amplitude of the resonance peaks of the dynamic susceptibility calculated in this approximation are much closer to the exact values of these characteristics. The advantage of the new self-consistent approach is demonstrated by the example of calculation of the dynamic susceptibility of waves in an inhomogeneous medium.

Keywords: self-consistent approximation, Green's functions, vertex corrections, inhomogeneities, correlations, dynamic susceptibility
Mathematics Subject Classification: 34B27, 47N20, 47N30

(Some figures may appear in colour only in the online journal)

1. Introduction: standard self-consistent approximation

We briefly recall the main stages of the introduction of the self-consistent approximation (SCA), widely used in physics for the approximate calculation of the Green's functions. At

the end of the 1950s to the beginning of the 1960s, this variant of SCA was introduced independently in different fields of physics. It was proposed by Migdal in the study of electron–phonon interaction [1], and then analyzed in detail in [2–5]. In those same years, a similar version of the SCA was independently proposed by Kraichnan [6] to investigate the effect of inhomogeneities on the dynamic susceptibility of waves in disordered media. A similar version was proposed to study the scattering of electrons in disordered media, as a generalization of the well known non-self-consistent Born approximation, and became known as the self-consistent Born approximation (see, e. g., [7, 8]).

It is well known [9–13] that the averaged Green's function $G(\mathbf{x}, \mathbf{x}_0)$ can be expressed through the vertex function $\Gamma(\mathbf{x}_1, \mathbf{x}_2; \mathbf{x}_3)$ (we omit the frequency ω from all expressions, where this does not lead to misunderstandings). To do this, consider the integral equation for the non-averaged Green's function $\tilde{G}(\mathbf{x}, \mathbf{x}_0)$

$$\tilde{G}(\mathbf{x}, \mathbf{x}_0) = g(\mathbf{x}, \mathbf{x}_0) + \gamma \int g(\mathbf{x}, \mathbf{x}')\rho(\mathbf{x}')\tilde{G}(\mathbf{x}', \mathbf{x}_0)\mathrm{d}\mathbf{x}', \tag{1}$$

where $\rho(\mathbf{x}')$ is a centered ($\langle\rho\rangle = 0$) and normalized ($\langle\rho^2\rangle = 1$) random function, γ is the rms fluctuation, and $g(\mathbf{x}, \mathbf{x}_0)$ is the original Green's function. A system of equations relating the averaged Green's function $G(\mathbf{x}, \mathbf{x}_0)$ and the vertex function derives from equation (1) by the methods of functional variation analysis in the form

$$G(\mathbf{x}, \mathbf{x}_0) = g(\mathbf{x}, \mathbf{x}_0) + \int\int g(\mathbf{x}, \mathbf{x}')\Sigma(\mathbf{x}', \mathbf{x}'')G(\mathbf{x}'', \mathbf{x}_0)\mathrm{d}\mathbf{x}'\mathrm{d}\mathbf{x}'', \tag{2}$$

$$\Sigma(\mathbf{x}', \mathbf{x}'') = \gamma^2 \int\int K(\mathbf{x}', \mathbf{x}_2)G(\mathbf{x}', \mathbf{x}_1)\Gamma(\mathbf{x}_1, \mathbf{x}''; \mathbf{x}_2)\mathrm{d}\mathbf{x}_1\mathrm{d}\mathbf{x}_2, \tag{3}$$

$$\begin{aligned}\Gamma(\mathbf{x}_1, \mathbf{x}''; \mathbf{x}_2) = \delta(\mathbf{x}_1 - \mathbf{x}_2)\delta(\mathbf{x}_1 - \mathbf{x}'') + \gamma^2 \int\int\int\int K(\mathbf{x}'', \mathbf{x}_3)\Gamma(\mathbf{x}_1, \mathbf{x}_4; \mathbf{x}_3)G(\mathbf{x}_4, \mathbf{x}_5) \\ \times \Gamma(\mathbf{x}_5, \mathbf{x}_6; \mathbf{x}_2)G(\mathbf{x}_6, \mathbf{x}'')\mathrm{d}\mathbf{x}_3\mathrm{d}\mathbf{x}_4\mathrm{d}\mathbf{x}_5\mathrm{d}\mathbf{x}_6 + \ldots.\end{aligned} \tag{4}$$

Here the Dyson equation (2) and the expression of the self-energy Σ in terms of the vertex function Γ, equation (3), are exact equations, and the expression for the vertex function Γ, equation (4), is an infinite series.

The parameter γ and the function $K(\mathbf{x}_i, \mathbf{x}_j)$ have different meanings for different physical problems. In the theory of electron–phonon interaction the function $K(\mathbf{x}_i, \mathbf{x}_j)$ is usually designated as $D(\mathbf{x}_i, \mathbf{x}_j)$ and the expression $\gamma^2 D(\mathbf{x}_i, \mathbf{x}_j)$ is the operator of the electron–phonon interaction, where γ^2 is proportional to the electron–phonon interaction parameter λ, and $D(\mathbf{x}_i, \mathbf{x}_j)$ is a normalized function ($D(\mathbf{x}_i, \mathbf{x}_i) = 1$). In the theory of scattering of waves or electrons in heterogeneous media, γ is the rms fluctuation of inhomogeneities and $K(\mathbf{x}_i, \mathbf{x}_j)$ is the normalized correlation function of these inhomogeneities ($K(\mathbf{x}', \mathbf{x}') = 1$). In the case of electron scattering the correlation function is the average sum of potentials of the interaction between electrons and impurities.

We use the Fourier transformation in the form used in solid state theory:

$$f(\mathbf{x}) = (2\pi)^{-\mathrm{d}} \int f(\mathbf{k})\mathrm{e}^{\mathrm{i}\mathbf{k}\mathbf{x}}\mathrm{d}\mathbf{k}, \tag{5}$$

$$f(\mathbf{k}) = \int f(\mathbf{x})\mathrm{e}^{-\mathrm{i}\mathbf{k}\mathbf{x}}\mathrm{d}\mathbf{x}, \tag{6}$$

where d is the dimensionality of space. In stochastic radio physics [12–18] and a number of other branches of science, the factor $1/(2\pi)^{\mathrm{d}}$ is usually transferred from equation (5) into

equation (6). This transfer leads to the appearance of this factor in the expressions for the Green's functions and Dyson equation and changes its degree in other terms in the momentum space.

The system of equations (2)–(4) in $\mathbf{k}$-space takes the form

$$G(\mathbf{k}, \mathbf{k}_0) = g(\mathbf{k}, \mathbf{k}_0) + (2\pi)^{-2d}\int\int g(\mathbf{k}, \mathbf{k}_1)\Sigma(-\mathbf{k}_1, \mathbf{k}_2)G(-\mathbf{k}_2, \mathbf{k}_0)\mathrm{d}\mathbf{k}_1\mathrm{d}\mathbf{k}_2, \tag{7}$$

$$\Sigma(-\mathbf{k}_1, \mathbf{k}_2) = \gamma^2(2\pi)^{-3\mathrm{d}}\iiint S(-\mathbf{k}_1 - \mathbf{q}_2, \mathbf{q}_1)G(\mathbf{q}_2, \mathbf{q}_3)\Gamma(-\mathbf{q}_3, \mathbf{k}_2; -\mathbf{q}_1)\mathrm{d}\mathbf{q}_1\mathrm{d}\mathbf{q}_2\mathrm{d}\mathbf{q}_3, \tag{8}$$

$$\begin{aligned}\Gamma(-\mathbf{q}_3, \mathbf{k}_2; -\mathbf{q}_1) &= (2\pi)^d\delta(\mathbf{k}_2 - \mathbf{q}_1 - \mathbf{q}_3) + \gamma^2(2\pi)^{-5d}\iiiint S(\mathbf{k}_2 - \mathbf{p}_5, \mathbf{p}_1)\\ &\times\Gamma(-\mathbf{q}_3, \mathbf{p}_2; -\mathbf{p}_1)G(-\mathbf{p}_2, \mathbf{p}_3)\Gamma(-\mathbf{p}_3, \mathbf{p}_4; -\mathbf{q}_1)G(-\mathbf{p}_4, \mathbf{p}_5)d\mathbf{p}_1d\mathbf{p}_2d\mathbf{p}_3d\mathbf{p}_4d\mathbf{p}_5,\end{aligned} \tag{9}$$

where $S(\mathbf{k}_1, \mathbf{k}_2)$ is the Fourier transform of the correlation function $K(\mathbf{x}_1, \mathbf{x}_2)$.

In the case of a spatially invariant medium, the transition from the two-point to the single-point functions and from the three-point to the two-point functions is performed using the formulas

$$G(\mathbf{k}_1, \mathbf{k}_2) = (2\pi)^{\mathrm{d}}G_{\mathbf{k}_2}\delta(\mathbf{k}_1 + \mathbf{k}_2), \tag{10}$$

$$\Gamma(\mathbf{k}_1, \mathbf{k}_2; \mathbf{k}_3) = (2\pi)^{\mathrm{d}}\Gamma_{\mathbf{k}_2,\mathbf{k}_3}\delta(\mathbf{k}_1 + \mathbf{k}_2 + \mathbf{k}_3). \tag{11}$$

The resulting system of equations (7)–(9) after a replacement of the integration variables can be reduced to the form

$$G_{\mathbf{k}} = g_{\mathbf{k}} + g_{\mathbf{k}}\Sigma_{\mathbf{k}}G_{\mathbf{k}}, \tag{12}$$

$$\Sigma_{\mathbf{k}} = \gamma^2(2\pi)^{-\mathrm{d}}\int S_{\mathbf{k}-\mathbf{k}_1}G_{\mathbf{k}_1}\Gamma_{\mathbf{k},\mathbf{k}-\mathbf{k}_1}\mathrm{d}\mathbf{k}_1, \tag{13}$$

$$\Gamma_{\mathbf{k},\mathbf{k}-\mathbf{k}_1} \approx 1 + \gamma^2(2\pi)^{-\mathrm{d}}\int S_{\mathbf{k}_1-\mathbf{k}_2}G_{\mathbf{k}_2}G_{\mathbf{k}-\mathbf{k}_1+\mathbf{k}_2}\Gamma_{\mathbf{k}_2,\mathbf{k}_1-\mathbf{k}_2}\Gamma_{\mathbf{k}-\mathbf{k}_1+\mathbf{k}_2,\mathbf{k}-\mathbf{k}_1}\mathrm{d}\mathbf{k}_2. \tag{14}$$

The Migdal, Kraichnan, and Born SCA corresponds to taking into account in equation (14) only the first term of the expansion, i.e., $\Gamma = 1$. Equations (12) and (13) form a closed system of equations in this case. The SCA corresponding to this system is applied in two different forms. The first form involves the exact representation of $G_{\mathbf{k}}$ in terms of the self-energy $\Sigma_{\mathbf{k}}$, resulting from the Dyson equation (12)

$$G_{\mathbf{k}} = \frac{1}{g_{\mathbf{k}}^{-1} - \Sigma_{\mathbf{k}}}, \tag{15}$$

and for $\Sigma_{\mathbf{k}}$ the approximate self-consistent equation is derived from equations (13) and (15)

$$\Sigma_{\mathbf{k}} \approx \gamma^2(2\pi)^{-\mathrm{d}}\int\frac{S_{\mathbf{k}-\mathbf{k}_1}\mathrm{d}\mathbf{k}_1}{g_{\mathbf{k}_1}^{-1} - \Sigma_{\mathbf{k}_1}}, \tag{16}$$

where $S_{\mathbf{k}}$ is the Fourier transform of the normalized correlation function $K(\mathbf{x}', \mathbf{x}'')$, the normalized interaction function $D(\mathbf{x}', \mathbf{x}'')$ or the average potential of the interaction between electrons and impurities.

To obtain the second form of the SCA, equation (13) is substituted into equation (12). This leads to the approximate nonlinear integral self-consistent equation for the Green's function $G_{\mathbf{k}}$

$$G_{\mathbf{k}} \approx \frac{1}{g_{\mathbf{k}}^{-1} - \gamma^2 (2\pi)^{-\mathrm{d}} \int S_{\mathbf{k}-\mathbf{k}_1} G_{\mathbf{k}_1} \mathrm{d}\mathbf{k}_1}. \tag{17}$$

The Migdal approximation, the Kraichnan approximation, and the self-consistent Born approximation were proposed for different physical problems. There are also mathematical differences between them: for example, the Born approximation, in contrast to the Migdal approximations and Kraichnan, takes into account both Gaussian and non-Gaussian components of the random field. At the same time, all these variants of the self-consistent approach have one common cardinal property: the expansion of the Green's function obtained by these methods contains all diagrams appearing in the exact expression for $G(\mathbf{x}, \mathbf{x}_0)$ except for the diagrams with intersecting interaction/correlation lines between different points. For the purposes of this work, this variant will be called below the standard self-consistent approximation. Lack of diagrams with intersecting line correlations, which the majority of the exact expression for $G(\mathbf{x}, \mathbf{x}_0)$, imposes restrictions on the range of applicability of the standard approximation and the accuracy of the results obtained with its help.

The role of the standard SCA is different when considering various physical problems. Thus, the accuracy of the standard SCA is sufficient for the study of many aspects of wave scattering by inhomogeneities [14–18]. However, calculation of the shape and width of the resonance line going beyond the standard SCA is required even in this problem. The scope of application of the standard SCA in the theory of electron–phonon interaction is much narrower: it can be used to calculate the self-energy only to the first order in λ. To calculate the temperature of the superconducting transition (especially for high-temperature superconductors) requires knowledge of the self-energy, at least in terms of second order. Therefore, intensive studies of amendments to the self-energy due to taking into account the next term in the expansion of the vertex function (vertex corrections) are carried out [19–28]. To take into account the vertex corrections, is developed a number of approaches that use the ladder approximation, the Ward identity, a simplified representation of the operator of the electron–phonon interaction, etc. A sequential overview of the main works carried out in this area, until 2000, is given in [26]. In [19–28] significant progress in the study of the vertex corrections has been achieved. However, the discrepancy between the results of the different approaches still remains significant.

Creating a new SCA, which takes into account both the first and second terms in the expansion of the vertex function, would contribute to the development of methods such as the scattering theory of waves and electrons, and the theory of electron–phonon interaction. This SCA would contain in the expression for the self-energy, in addition to all diagrams with non-intersecting lines of interaction/correlation, a significant number of diagrams with intersections of these lines. The derivation of this SCA is the purpose of this work.

2. Derivation of the new SCA

The idea of deriving self-consistency equations, which will be developed by us below, has been applied to the system of equations (2)–(4) and did not lead to the goal, for reasons which will be described below. Therefore, the first step in realization of this idea is to derive an alternative system of equations to (2)–(4). To do this in the original integral equation for the Green's function (1) we swap the functions g and $\tilde{G}$ in the integrand and write this equation in the form

$$\tilde{G}(\mathbf{x}, \mathbf{x}_0) = g(\mathbf{x}, \mathbf{x}_0) + \gamma \int \tilde{G}(\mathbf{x}, \mathbf{x}')\rho(\mathbf{x}')g(\mathbf{x}', \mathbf{x}_0)\mathrm{d}\mathbf{x}'. \tag{18}$$

Equations (1) and (18) are equivalent to each other because by an iterative process they lead to the same series of the Green's function. Then we carry out with equation (18) the same functional operations that were carried out in [9–13] with equation (1) (see appendix A). The result is that the system of equations, an alternative to system (2)–(4), has the form

$$G(\mathbf{x}, \mathbf{x}_0) = g(\mathbf{x}, \mathbf{x}_0) + \int\int G(\mathbf{x}, \mathbf{x}')\Sigma(\mathbf{x}', \mathbf{x}'')g(\mathbf{x}'', \mathbf{x}_0)\mathrm{d}\mathbf{x}'\mathrm{d}\mathbf{x}'', \tag{19}$$

$$\Sigma(\mathbf{x}', \mathbf{x}'') = \gamma^2 \int\int \Gamma(\mathbf{x}', \mathbf{x}_1; \mathbf{x}_2)K(\mathbf{x}_2, \mathbf{x}'')G(\mathbf{x}_1, \mathbf{x}'')\mathrm{d}\mathbf{x}_1\mathrm{d}\mathbf{x}_2, \tag{20}$$

$$\begin{aligned}\Gamma(\mathbf{x}', \mathbf{x}_1; \mathbf{x}_2) \approx \delta(\mathbf{x}' - \mathbf{x}_2)\delta(\mathbf{x}' - \mathbf{x}_1) + \gamma^2 \int\int\int\int K(\mathbf{x}_1, \mathbf{x}_4)\Gamma(\mathbf{x}', \mathbf{x}_3; \mathbf{x}_4)G(\mathbf{x}_3, \mathbf{x}_5) \\ \times \Gamma(\mathbf{x}_5, \mathbf{x}_6; \mathbf{x}_2)G(\mathbf{x}_6, \mathbf{x}_1)\mathrm{d}\mathbf{x}_3\mathrm{d}\mathbf{x}_4\mathrm{d}\mathbf{x}_5\mathrm{d}\mathbf{x}_6.\end{aligned} \tag{21}$$

Performing the Fourier transformation of these equations, and then transferring via equations (10) and (11) to a spatially invariant medium, we obtain

$$G_{\mathbf{k}} = g_{\mathbf{k}} + g_{\mathbf{k}}\Sigma_{\mathbf{k}}G_{\mathbf{k}}, \tag{22}$$

$$\Sigma_{\mathbf{k}} = \gamma^2(2\pi)^{-\mathrm{d}} \int S_{\mathbf{k}-\mathbf{k}_1} G_{\mathbf{k}_1} \Gamma_{\mathbf{k}_1,\mathbf{k}-\mathbf{k}_1} \mathrm{d}\mathbf{k}_1, \tag{23}$$

$$\Gamma_{\mathbf{k}_1,\mathbf{k}-\mathbf{k}_1} \approx 1 + \gamma^2(2\pi)^{-\mathrm{d}} \int S_{\mathbf{k}-\mathbf{q}} G_{\mathbf{q}} G_{\mathbf{q}-\mathbf{k}+\mathbf{k}_1} \Gamma_{\mathbf{q},\mathbf{k}-\mathbf{q}} \Gamma_{\mathbf{q}-\mathbf{k}+\mathbf{k}_1,\mathbf{k}-\mathbf{k}_1} \mathrm{d}\mathbf{q}. \tag{24}$$

Next, we transform the system of equations (22)–(24) by substituting equation (24) into equation (23) and redesignating variables of integration in the last term of this equation, $\mathbf{q} \to \mathbf{k}_1$, $\mathbf{k}_1 \to \mathbf{q}$

$$\begin{aligned}\Sigma_{\mathbf{k}\,\mathrm{app}} \approx \gamma^2(2\pi)^{-\mathrm{d}} \int S_{\mathbf{k}-\mathbf{k}_1} G_{\mathbf{k}_1} \mathrm{d}\mathbf{k}_1 + \gamma^4(2\pi)^{-2\mathrm{d}} \int\int S_{\mathbf{k}-\mathbf{k}_1} S_{\mathbf{k}-\mathbf{q}} G_{\mathbf{k}_1} G_{\mathbf{q}} G_{\mathbf{k}_1-\mathbf{k}+\mathbf{q}} \Gamma_{\mathbf{k}_1,\mathbf{k}-\mathbf{k}_1} \\ \times \Gamma_{\mathbf{k}_1-\mathbf{k}+\mathbf{q},\mathbf{k}-\mathbf{q}} \mathrm{d}\mathbf{k}_1\mathrm{d}\mathbf{q}.\end{aligned} \tag{25}$$

We still have a system of three equations, but instead of equation (24) therein, along with the exact equations (22) and (23), equation (25) appears as an approximation. Let us change the variable of integration in the last term of equation (25), $\mathbf{q} = \mathbf{k} - \mathbf{k}_1 + \mathbf{k}_2$, $\mathrm{d}\mathbf{q} = \mathrm{d}\mathbf{k}_2$. As a result, equation (25) takes the form

$$\begin{aligned}\Sigma_{\mathbf{k}\,\mathrm{app}} \approx \gamma^2(2\pi)^{-\mathrm{d}} \int S_{\mathbf{k}-\mathbf{k}_1} G_{\mathbf{k}_1} \left[1 + \gamma^2(2\pi)^{-\mathrm{d}} \Gamma_{\mathbf{k}_1,\mathbf{k}-\mathbf{k}_1} \int S_{\mathbf{k}_1-\mathbf{k}_2} G_{\mathbf{k}_2} G_{\mathbf{k}-\mathbf{k}_1+\mathbf{k}_2} \Gamma_{\mathbf{k}_2,\mathbf{k}_1-\mathbf{k}_2} \mathrm{d}\mathbf{k}_2\right] \\ \times \mathrm{d}\mathbf{k}_1.\end{aligned} \tag{26}$$

Equations (23) and (26) in diagram form are shown in figure 1(a). Figure 1(b) shows for comparison diagrammatic equations that would be obtained if we used the usual form of the original equations (2)–(4). It is seen that in the latter case the functions Γ (circles) have different internal structures of the wave vector combinations. In figure 1(a) the structure of all functions Γ is uniform. This allows us to take the final step to obtain a system of self-consistent equations. Equation (23) includes an exact value of the vertex function $\Gamma_{\mathbf{k}_1,\mathbf{k}-\mathbf{k}_1}$. In

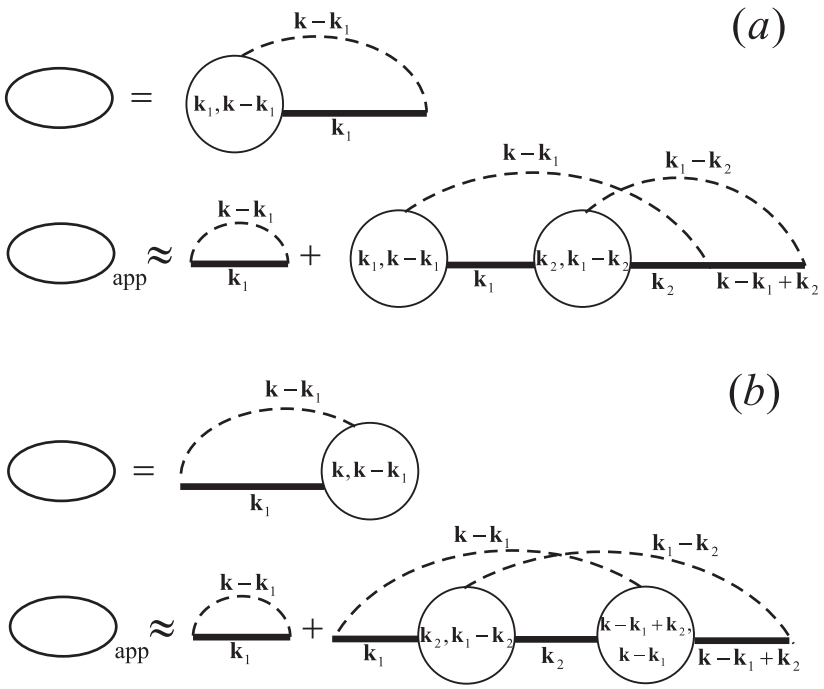

Figure 1. Diagram representations for $\Sigma_{\mathbf{k}}$ and $\Sigma_{\mathbf{k}\mathrm{app}}$ which follow from equations (23) and (26) (*a*) and from equations (12) and (14) (*b*).

equation (26) the expression in brackets corresponds to the approximate value of the same function. Equating these two expressions to each other, we obtain an approximate equation

$$\int S_{\mathbf{k}-\mathbf{k}_1} G_{\mathbf{k}_1} \left\{ \Gamma_{\mathbf{k}_1,\mathbf{k}-\mathbf{k}_1} - \left[1 + \gamma^2 (2\pi)^{-\mathrm{d}} \Gamma_{\mathbf{k}_1,\mathbf{k}-\mathbf{k}_1} \int S_{\mathbf{k}_1-\mathbf{k}_2} G_{\mathbf{k}_2} G_{\mathbf{k}-\mathbf{k}_1+\mathbf{k}_2} \Gamma_{\mathbf{k}_2,\mathbf{k}_1-\mathbf{k}_2} \mathrm{d}\mathbf{k}_2 \right] \right\} \times d\mathbf{k}_1 \approx 0. \tag{27}$$

Under the integral sign in $\mathbf{k}_1$ in equation (27) is the difference of two functions that depend on the same parameter $\mathbf{k}$. Since the difference of the integrals of these functions must be zero for all values of this parameter and the product of $S_{\mathbf{k}-\mathbf{k}_1} G_{\mathbf{k}_1} \neq 0$, the vanishing of the expression in curly brackets is implied from equation (27). From this expression we obtain a self-consistent equation for the vertex function $\Gamma_{\mathbf{k}_1,\mathbf{k}-\mathbf{k}_1}$, which is conveniently written in the form

$$\Gamma_{\mathbf{k}_1,\mathbf{k}-\mathbf{k}_1} \approx \frac{1}{1 - \gamma^2 (2\pi)^{-\mathrm{d}} \int S_{\mathbf{k}_1-\mathbf{k}_2} G_{\mathbf{k}_2} G_{\mathbf{k}-\mathbf{k}_1+\mathbf{k}_2} \Gamma_{\mathbf{k}_2,\mathbf{k}_1-\mathbf{k}_2} \mathrm{d}\mathbf{k}_2}. \tag{28}$$

Replacing in equations (23) and (28) the Green's functions of their representations through the self-energies from the Dyson equation (22), we obtain the general form of a system of two integral equations of the new self-consistent approximation

$$\Sigma_{\mathbf{k}} = \gamma^2 (2\pi)^{-\mathrm{d}} \int \frac{S_{\mathbf{k}-\mathbf{k}_1} \Gamma_{\mathbf{k}_1,\mathbf{k}-\mathbf{k}_1} \mathrm{d}\mathbf{k}_1}{g_{\mathbf{k}_1}^{-1} - \Sigma_{\mathbf{k}_1}}, \tag{29}$$

$$\Gamma_{\mathbf{k}_1,\mathbf{k}-\mathbf{k}_1} \approx \frac{1}{1 - \gamma^2(2\pi)^{-\mathrm{d}}\int \frac{S_{\mathbf{k}_1-\mathbf{k}_2}\Gamma_{\mathbf{k}_2,\mathbf{k}_1-\mathbf{k}_2}\mathrm{d}\mathbf{k}_2}{[g^{-1}_{\mathbf{k}_2} - \Sigma_{\mathbf{k}_2}][g^{-1}_{\mathbf{k}-\mathbf{k}_1+\mathbf{k}_2} - \Sigma_{\mathbf{k}-\mathbf{k}_1+\mathbf{k}_2}]}}. \tag{30}$$

From this system, the self-energy $\Sigma_{\mathbf{k}}$ and the vertex function $\Gamma_{\mathbf{k}_1,\mathbf{k}-\mathbf{k}_1}$ can be expressed in terms of the original Green's function $g_{\mathbf{k}}$ and the spectral density of inhomogeneities $S_{\mathbf{k}}$. Depending on the task type the function $S_{\mathbf{k}}$ (together with the parameter γ^2) describes the correlations of inhomogeneities or interaction forces. Equations of the new SCA can be rewritten also in another form. For this, we substitute equation (23) into equation (22), and use equation (28) as the second equation. Then the system of integral equations of the new SCA takes the form

$$G_{\mathbf{k}} = \frac{1}{g^{-1}_{\mathbf{k}} - \gamma^2(2\pi)^{-\mathrm{d}}\int S_{\mathbf{k}-\mathbf{k}_1} G_{\mathbf{k}_1}\Gamma_{\mathbf{k}_1,\mathbf{k}-\mathbf{k}_1}\mathrm{d}\mathbf{k}_1}, \tag{31}$$

$$\Gamma_{\mathbf{k}_1,\mathbf{k}-\mathbf{k}_1} \approx \frac{1}{1 - \gamma^2(2\pi)^{-\mathrm{d}}\int S_{\mathbf{k}_1-\mathbf{k}_2} G_{\mathbf{k}_2} G_{\mathbf{k}-\mathbf{k}_1+\mathbf{k}_2}\Gamma_{\mathbf{k}_2,\mathbf{k}_1-\mathbf{k}_2}\mathrm{d}\mathbf{k}_2}. \tag{32}$$

For various tasks, the first, equations (29) and (30), or the second, equations (31) and (32), system may be preferred. In both cases, the self-consistency equations can be represented as a system of two coupled continued fractions with integral terms (or, respectively, as a system of two recurrence formulas for $\Sigma^{(n)}_{\mathbf{k}}$ and $\Gamma^{(m)}_{\mathbf{k}_1,\mathbf{k}-\mathbf{k}_1}$, or $G^{(n)}_{\mathbf{k}}$, and $\Gamma^{(m)}_{\mathbf{k}_1,\mathbf{k}-\mathbf{k}_1}$ ($n, m = 1, 2, 3, ...$), in the same way as done for $\Sigma^{(n)}_{\mathbf{k}}$ in the case of a standard approach [17, 18].

3. Investigation of the new SCA

Next we investigate the system of equations of the new approach and illustrate its advantages. This SCA contains all the lower-level approximations. Neglecting in the denominator of equation (30) or equation (32) a term of the order γ^2 we would get $\Gamma_{\mathbf{k}_1,\mathbf{k}-\mathbf{k}_1} \equiv 1$. Substituting this value in equation (29) or equation (31) turns each of them into the equation of the standard SCA, equation (16) or equation (17), respectively. If in equation (29) we set $\Sigma_{\mathbf{k}}$ in the denominator equal to zero, along with $\Gamma_{\mathbf{k}_1,\mathbf{k}-\mathbf{k}_1} \equiv 1$, we obtain the equation (not self-consistent) of the Bourret approximation [29, 30].

We carry out a comparison of the results of the new and standard SCAs on the simplest model of the wave equation in a randomly inhomogeneous medium

$$\nabla^2\varphi + [\nu + \gamma\rho(\mathbf{x})]\varphi = 0. \tag{33}$$

Both parameters, ν and γ, included in equation (33) are normalized to the dimensionality of a square of a wave number. For scalar models of electromagnetic or elastic waves $\nu = (\omega/s)^2$, where ω is the frequency, s is the velocity of corresponding waves in the medium; for spin waves $\nu = (\omega - \omega_0)/g\alpha M$, ω_0 is the frequency of the uniform ferromagnetic resonance, g is the gyromagnetic ratio, α is the exchange parameter, and M is the magnetization. In all cases, γ is the rms fluctuation of the corresponding inhomogeneities. We consider the case of one-dimensional inhomogeneities and model the stochastic properties of the random function $\rho(x)$ by exponential correlations:

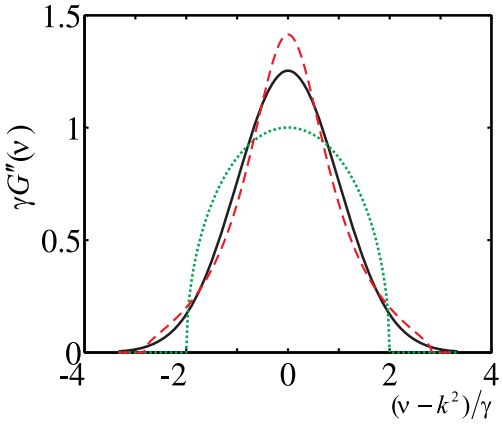

Figure 2. The imaginary part of the Green's function at $k_c = 0$ for the cases of the standard SCA, equation (37) (green dotted curve), the new SCA, equation (38) (red dashed curve), and the exact summation of all diagrams, equation (36) (solid black curve).

$$K(r) = e^{-k_c|x-x'|},\ S_k = \frac{2k_c}{k_c^2 + k^2}, \tag{34}$$

where k_c is the correlation wave number ($r_c = k_c^{-1}$ is the correlation radius of the inhomogeneities). The original Green's function in this case is

$$g_{\mathbf{k}} = \frac{1}{\nu - k^2}. \tag{35}$$

3.1. The limit of infinite correlation radius ($k_c = 0$)

Analytical study of self-consistent equations for this problem is possible in the limiting case, which corresponds to $k_c \to 0$ and, correspondingly, $S_{k-k_1} \to 2\pi\delta(k - k_1)$. In this case the series for the Green's functions can be summed up exactly (Keldysh model, see book [8]) and the imaginary part of the Green's function is

$$G''(\nu, k) = \pi e^{-\xi^2/2\gamma^2}/(2\pi)^{1/2}\gamma,\ \xi = \nu - k^2. \tag{36}$$

Integral equations of the standard SCA, equations (16) or (17), in the case $k_c \to 0$ also to be solved exactly [17]:

$$G''_{\text{sta}}(\nu, k) = \begin{cases} [(2\gamma)^2 - \xi^2]^{1/2}/2\gamma^2, & |\xi| \leqslant 2\gamma, \\ 0, & |\xi| > 2\gamma. \end{cases} \tag{37}$$

Equations of the system (29) and (30) or (31) and (32) in the case $k_c \to 0$ are reduced to a system of algebraic equations. After exclusion of the function Γ_k of this system, we obtain the quadratic equation for Σ_k (or G_k), from which we find

$$G''_{\text{new}}(\nu, k) = \begin{cases} [8\gamma^2 - \xi^2]^{1/2}/2(\xi^2 + \gamma^2), & |\xi| \leqslant 2.8\gamma, \\ 0, & |\xi| > 2.8\gamma. \end{cases} \tag{38}$$

Earlier [17], we compared equations (36) and (37) with each other. Let us compare all three equations, (36), (37), and (38). The corresponding curves $G''(\nu, k)$ are shown in

figure 2. It is seen that the new approach much better reflects the shape, linewidth, and amplitude of the resonance curve.

In the limiting case $k_c = 0$ the number of diagrams in the expansion of the Green's function for each SCA version can also be found analytically. It is known that the exact representation of the Green's function in this case has the form (see, e.g., [7, 8])

$$G = g\sum_{n=0}^{\infty} B_n z^n, \tag{39}$$

where $B_n = (2n-1)!!$, $z = \gamma^2 g^2$, $n = 0,\ \ 1,\ \ 2,\ \ 3....$

Consider the Green function G_{sta}, as determined by equation (17) for the standard SCA. The solution of a quadratic equation, that follows from equation (17) for the limiting case $k_c \to 0$, is

$$G_{sta} = gW, \tag{40}$$

where

$$W = \frac{1-\sqrt{1-4z}}{2z}. \tag{41}$$

Expanding the generating function (41) in the binomial series [31], we obtain

$$G_{sta} = g\sum_{n=0}^{\infty} C_n z^n, \tag{42}$$

where $C_n = \frac{(2n)!}{n!\,(n+1)!}$ are Catalan numbers.

Now consider the function G_{new}, for which the system of equations (31) and (32) at $k_c \to 0$ is also reduced to a quadratic equation. Its solution can be represented in the form

$$G_{new} = gX, \tag{43}$$

where

$$X = \frac{3-\sqrt{1-8z}}{2(1+z)}. \tag{44}$$

We rewrite the generating function (44) in the form

$$X = \frac{3}{2x}\left[1-\sqrt{1-\frac{8}{9}x}\right], \tag{45}$$

where $x = 1 + z$. Expanding the square root in the binomial series

$$X = \frac{3}{2x}\left[1-\sum_{m=0}^{\infty}\left(-\frac{8}{9}x\right)^m\binom{1/2}{m}\right], \tag{46}$$

and using the formula

$$\binom{1/2}{m} = \frac{(-1)^{m-1}}{(2m-1)4^m}\frac{(2m)!}{[m!]^2}, \tag{47}$$

we obtain

$$X = \frac{3}{2x}\left[1+\sum_{m=0}^{\infty}\frac{2^m x^m}{3^{2m}(2m-1)}\frac{(2m)!}{[m!]^2}\right]. \tag{48}$$

Table 1. Number of diagrams in each order n of the expansion of the Green's function for the first six orders, taken into account in the standard SCA (G_{sta}), in the new SCA (G_{new}), and in the exact expression for the Green's function (G).

n	1	2	3	4	5	6
G_{sta}	1	2	5	14	42	132
G_{new}	1	3	13	67	381	2307
G	1	3	15	105	945	10 395

Transform the expression (48):

$$X = \sum_{m=1}^{\infty} \frac{2^{m-1}x^{m-1}}{3^{2m-1}(2m-1)} \frac{(2m)!}{(m!)^2} = \sum_{m=0}^{\infty} \frac{2^m x^m}{3^{2m+1}(2m+1)} \frac{(2m+2)!}{[(m+1)!]^2} = \sum_{m=0}^{\infty} \frac{2^{m+1}x^m}{3^{2m+1}} \times \frac{(2m)!}{(m+1)!m!}. \tag{49}$$

Expand x^m in the binomial series:

$$x^m = (1+z)^m = \sum_{n=0}^{\infty} \frac{m!}{(m-n)!n!} z^n. \tag{50}$$

Substituting (50) into (49) and (49) into (43), we obtain

$$G_{new} = g \sum_{n=0}^{\infty} S_n z^n, \tag{51}$$

where $S_n = \sum_{m=0}^{\infty} \frac{2^{m+1}(2m)!}{3^{2m+1}(m+1)!(m-n)!n!}$, $m = 0, \quad 1, \quad 2, \quad 3....$

Coefficients before z^n in sums included in expressions for the Green's functions (39), (42), (51) are a number of diagrams in each order n of the expansion of Green's functions in series. Table 1 shows the values of these numbers up to sixth order. The table shows that for $n > 1$ the new approach takes into account in every order n of the expansion of the Green function more diagrams than the standard SCA. Hence, the advantage of the new over the standard approach increases with increasing n. However, the number of diagrams in the exact expression (39) increases more rapidly. So, it is interesting to compare the relative contributions of both standard and new approximations to the total number of accurate diagrams in each order n of the expansion of G. Charts of such contributions are shown in figure 3, which shows relative portions (as percentages) of the number of exact diagrams taken into account by the new and the standard SCA. It is evident that, if the standard SCA accurately takes into account only the first order, the new accurately takes into account both the first and second order. In the following orders of the expansion the new SCA is also much closer to the exact value than the standard SCA. For example, at $n = 5$, the new SCA accounts for 40.3% of diagrams of the exact expression (39), and the standard SCA only 4.4%.

Let us calculate in the limiting case $k_c = 0$ also the number of diagrams in the expansion of the self-energy for the standard and the new SCA. The self-energy Σ_{sta} for the standard SCA is given by equation (16), that in the limiting case $k_c \to 0$ reduces to a quadratic equation, the solution of which is as follows:

$$\Sigma_{sta} = \gamma^2 g W, \tag{52}$$

where W is the generating function (41) and its expansion in a binomial series has formally the same form as in the expression (42). However, the index of summation in this series does not correspond to the order of the self-energy expansion in powers of γ^2, since expression

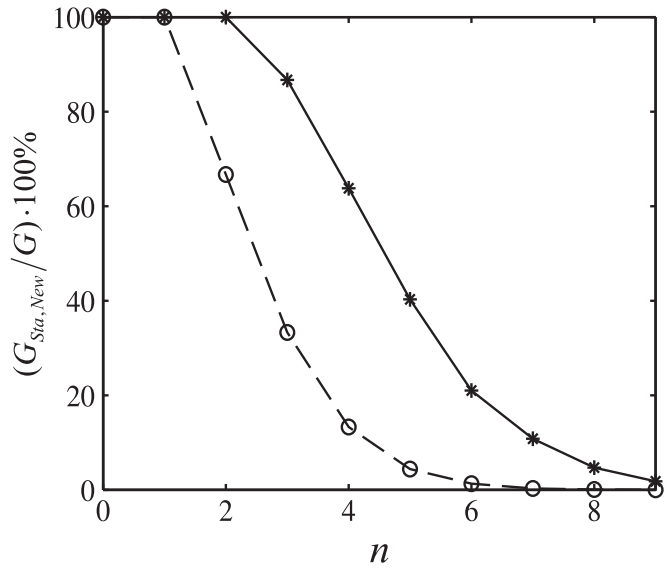

Figure 3. The relative proportions of the exact number of diagrams (in percent) accounted for in the standard (circles) and the new (asterisks) SCA in each term n of the expansion of the Green's function.

Table 2. Number of diagrams in each order n of expansion of the self-energy for the first six orders, taken into account in the standard (C_{n-1}) and the new (P_{n-1}) SCAs, and number of diagrams with intersecting correlations in the new SCA (N_{n-1}).

n	1	2	3	4	5	6
C_{n-1}	1	1	2	5	14	42
P_{n-1}	1	2	8	40	224	1344
N_{n-1}	0	1	6	35	210	1302

(52) differs from expression (40) by a factor γ^2. In order to retain for the index n the sense of the order of expansion, the expression (52) should be written in the form

$$\Sigma_{\text{sta}} = \gamma^2 g \sum_{n=1}^{\infty} C_{n-1} z^{n-1}, \tag{53}$$

where $C_{n-1} = \frac{(2n-2)!}{(n-1)!\,(n)!}$ are Catalan numbers, $n = 1,\ 2,\ 3....$

Consider the self-energy for the new SCA. The function Σ_{new} is determined by the system of equations (29) and (30), which reduces to a quadratic equation when $k_c \to 0$. Its solution has the form

$$\Sigma_{\text{new}} = \gamma^2 g\,[1 - \sqrt{1-8z}\,]/(4z). \tag{54}$$

Expanding the square root in the binomial series, and using (47), we obtain

$$\Sigma_{\text{new}} = \gamma^2 g \sum_{n=1}^{\infty} P_{n-1} z^{n-1}, \tag{55}$$

where $P_{n-1} = \frac{2^{n-1}(2n-2)!}{(n-1)!\,n!}$.

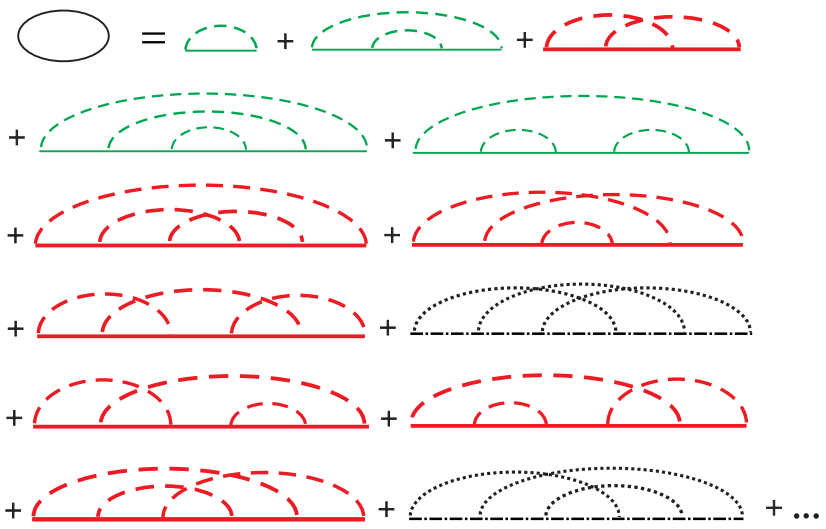

Figure 4. Diagram representation of the mass operator $\Sigma_{\mathbf{k}}$ (first three orders of its expansion) in terms of the original Green's functions $g_{\mathbf{k}}$ for the cases of the standard (thin green lines) and the new (thin green lines + thick red lines) approximations. Diagrams unaccounted for in the new approximation are shown by dot–dashed (Green's functions $g_{\mathbf{k}}$) and dotted (correlations) lines.

The coefficients C_{n-1} and P_{n-1} in expressions (53) and (55) represent the number of diagrams in each order n of the expansion in series of the self-energy. Table 2 shows the values of these numbers to the sixth order for a standard (first row) and the new (second row) SCA. The table shows that the new approach for $n > 1$ takes into account in every order n of expansion of the self-energy more diagrams than the standard SCA. Hence, the advantage of the new approach over the standard one increases with increasing n.

3.2. The arbitrary correlation radius ($k_c \neq 0$)

We considered in the previous section the number of diagrams contained in each order of a series expansion of the Green's function G, and the self-energy Σ, found in both the standard and the new approach when $k_c = 0$. In the general case of an arbitrary radius correlation ($k_c \neq 0$) the number of diagrams is determined by the same formulas (42), (51), (53) and (55). Moreover, the number of diagrams with non-intersecting and intersecting lines of correlation/interaction, which is contained in each order of the series expansion of the self-energy Σ, can also be found by formulas (53) and (55). The coefficient C_{n-1} in formula (53), which takes into account the total number of diagrams for the standard SCA, also determines the number of diagrams with non-intersecting lines of correlation for the new SCA. Accordingly, the number of diagrams with intersecting lines of correlation for the new SCA is determined by the difference between the coefficients P_{n-1} and C_{n-1}:

$$N_{n-1} = P_{n-1} - C_{n-1} = C_{n-1}(2^{n-1} - 1). \tag{56}$$

Thus, table 2 illustrates not only the advantage of the new SCA over the standard one, but also the number of diagrams with non-intersecting (first row) and intersecting (third row) lines of correlation/interaction taken into account in the new approach.

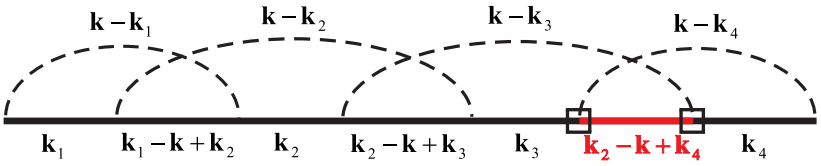

Figure 5. One of the two defective diagrams of the fourth order. Points of violation of the law of conservation of momentum are shown by squares. There is the Green's function $G_{k_2-k+k_4}$ between them instead of $G_{k_3-k+k_4}$.

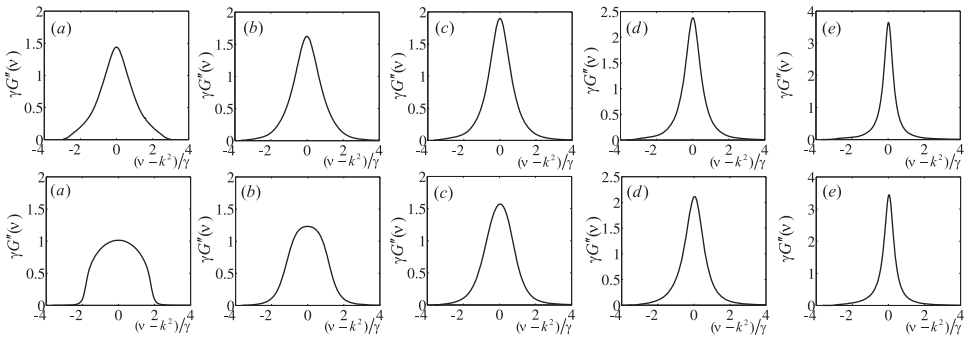

Figure 6. The imaginary part of the Green's function calculated in the new SCA (top row of graphs) and in the standard SCA (bottom row) at $u_c = k_c/\sqrt{\gamma} = 0.018$ (*a*), 0.18 (*b*), 0.33 (*c*), 0.5 (*d*), and 1.0 (*e*).

Let us consider in more detail the form of diagrams, which the new approach includes in the first three orders of expansion of the self-energy Σ_k in a series. For this, we expand in a series the equations (29) and (30) to terms of third order (i.e. to γ^6), and then iterate them to the same order. Figure 4 shows all diagrams included in the first three orders of the exact expression for the self-energy (13 diagrams). The new SCA takes into account 11 of them. Four of them are also taken into account in the standard SCA, and are shown in figure 4 as thin green lines; the remaining nine are depicted as thick red lines. Thus, the new SCA accurately describes the first and second orders (one and two diagrams, respectively) and includes eight to ten of diagrams of the third order in accordance with table 2.

The fourth and higher orders of expansion of the self-energy in a series, along with accurate diagrams, contain some faulty diagrams, which violate the law of conservation of momentum. An example of one such diagram is shown in figure 5. It differs from the accurate diagram by replacement of the Green's function $G_{k_3-k+k_4}$ by the Green's function $G_{k_2-k+k_4}$. This has led to a violation of the law of conservation of momentum at two points marked by squares in the figure. The appearance of such defective diagrams is associated with approximations used in the derivation of the new SCA. Estimates show that the effect of the defective diagrams on the final result of the calculation should be negligible. Thus, of the 40 diagrams taken into account in the fourth order, only two are defective. Of the seven Green's functions included in each diagram, one function in a defective diagram is incorrect. Therefore, from the 280 Green's functions taken into account in the fourth order, only two are incorrect. When $k_c \to 0$, all defective diagrams are transformed into accurate ones.

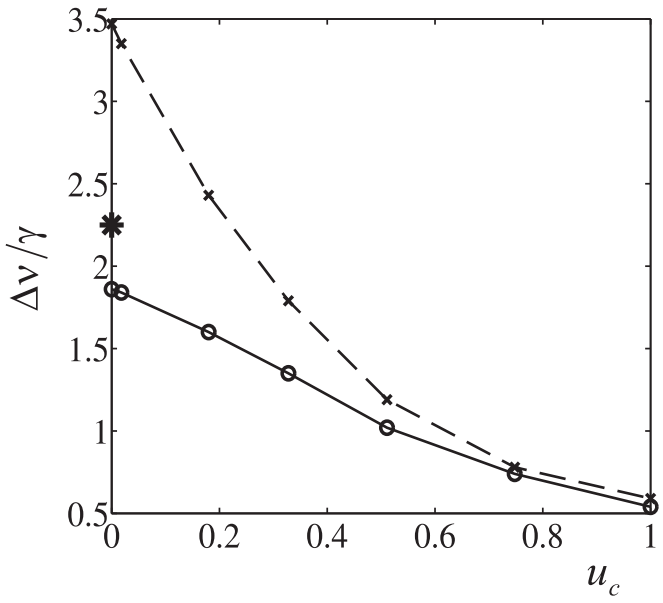

Figure 7. The linewidth $\Delta\nu$ of the resonance curve $G''(\nu)$ versus $u_c = k_c/\sqrt{\gamma}$ calculated in the improved SCA (circles) and in the standard SCA (crosses). The exact value of linewidth at $u_c = 0$ is also shown (asterisk).

Next, we compare the shape and linewidth of the $G''(\omega)$ resonance pick calculated in the framework of the new and standard approximation. The calculation is performed for the fixed wave number $k/\sqrt{\gamma} = 1.8$. Changing the shape of the function $G_k(\nu)$ with an increase in the dimensionless correlation wave number $u_c = k_c/\sqrt{\gamma}$, calculated in the framework of the new SCA, is shown in figure 6 (top row of graphs). Note that the scales of figures 6(d) and (e) are different from each other as well as that of figures 6(a)–(c). Changing the shape of the function $G_k''(\nu)$ with increasing u_c, calculated by us in the standard SCA, is also shown in figure 6 (bottom row of graphs). Figure 7 shows the variation in width of the resonance peak $\Delta\nu$ of the function $G_k''(\nu)$ with increasing u_c. Crosses in this figure correspond to the standard SCA, and circles to the new SCA. Compare the results obtained in the standard and the new SCA (figures 2, 6 and 7). In both cases, the widest resonance peak corresponds to the smallest value of u_c. A significant narrowing of the resonance peak and change in its shape occur with increasing u_c. The height of the peak increases, and its wings become unbounded. We now turn to the differences between the results obtained using the standard and the new SCA. It is seen from figures 2, 6 and 7 that the standard SCA is unsatisfactory to reproduce either the shape or width of the resonance peak of the function $G_k''(\nu)$ in most of the investigated range $0 \leqslant u_c \leqslant 1$. The most pronounced advantage of the new SCA over the standard SCA is shown for $u_c = 0$. In this case, we can compare the form of the resonance peaks calculated in different approximations with the known exact (Gaussian) form of this peak (figure 2). The shape of the resonance peak calculated in the standard SCA has, far from reality, a domed appearance; the peak width is much greater than the width of the exact resonance peak. In contrast, the resonance peak of the function $G_k''(\nu)$ calculated using the new SCA is similar to the exact peak in form and width. When u_c is different from zero, the advantage of the improved SCA over the standard SCA is manifested in a significant part of the investigated interval of u_c (figures 6 and 7). Whereas the distorted dome shape of the resonance peak

calculated in the standard SCA is manifested in varying degrees to all $u_c < 0.3$, the peak calculated in the new SCA has the usual resonance form over the entire range. Near the right-hand edge of the investigated interval, the results obtained when using both the new and standard approximations approach each other.

4. Conclusion

We summarize and discuss briefly the results obtained. A self-consistent approximation of a higher level compared to the standard self-consistent approximation is derived taking into account both the first and second terms of the series for the vertex function. In contrast to the standard approximation, a new self-consistent approximation is described by a system of two coupled nonlinear integral equations for the Green's function and the vertex function. In addition to all the diagrams with non-intersecting lines of correlation/interaction taken into account by the standard self-consistent approximation, the new approach takes into account in each term of the Green's function expansion a significant number of diagrams with intersections of these lines. Analytical formulas for the number of diagrams in each order of the expansion of both the Green function and self-energy for the standard and for the new approach have been derived. Tables and graphs that are based on these formulas demonstrate the advantage of the new approach. A comparison of the new and standard approximations was also carried out on a model problem of the dynamic susceptibility of waves in an inhomogeneous medium. The obtained results suggest that the new approach has undoubted advantages in the study of problems of both stochastic radio physics and optics in media with enough long-wave inhomogeneities ($k_c \ll k$), because it better describes the shape, line-width, and amplitude of the resonance lines than the standard approach. The proposed approach could be also applied in other areas of physics (the scattering of electrons on impurities, electron–phonon interaction, etc). The usefulness and limits of applicability of the new SCA in these areas require special studies which are beyond the scope of this paper.

Appendix A

Adding to the random function $\rho(\mathbf{x})$ in equation (18) the arbitrary deterministic function $\eta(\mathbf{x})$, we obtain

$$\tilde{G}(\mathbf{x}, \mathbf{x}_0; \gamma\rho(\tilde{\mathbf{x}}) + \eta(\tilde{\mathbf{x}})) = g(\mathbf{x}, \mathbf{x}_0) + \int \tilde{G}(\mathbf{x}, \mathbf{x}'; \gamma\rho(\tilde{\mathbf{x}}) + \eta(\tilde{\mathbf{x}}))[\gamma\rho(\mathbf{x}') + \eta(\mathbf{x}')] \times g(\mathbf{x}', \mathbf{x}_0)d\mathbf{x}'. \tag{A1}$$

By averaging of equation (A1) we obtain

$$G(\mathbf{x}, \mathbf{x}_0; \eta) = g(\mathbf{x}, \mathbf{x}_0) + \int G(\mathbf{x}, \mathbf{x}'; \eta)\eta(\mathbf{x}')g(\mathbf{x}', \mathbf{x}_0)d\mathbf{x}' + \gamma\int \langle \rho(\mathbf{x}')\tilde{G}(\mathbf{x}, \mathbf{x}'; \eta)\rangle \times g(\mathbf{x}', \mathbf{x}_0)d\mathbf{x}'. \tag{A2}$$

Then we decouple the average of the product $\rho\tilde{G}$ using the Furutsu–Novikov formula [32, 33]

$$\langle \rho(\mathbf{x}')\tilde{G}(\mathbf{x}, \mathbf{x}'; \eta)\rangle = \gamma \int K(\mathbf{x}', \mathbf{x}'') \frac{\delta G(\mathbf{x}, \mathbf{x}'; \eta)}{\delta \eta(\mathbf{x}'')}, \tag{A3}$$

where $K(\mathbf{x}', \mathbf{x}'')$ is the normalized correlation function

$$K(\mathbf{x}', \mathbf{x}'') = \langle \rho(\mathbf{x}')\rho(\mathbf{x}'')\rangle,\ K(\mathbf{x}', \mathbf{x}') = 1. \tag{A4}$$

To find the variational derivative in equation (A3) we use the identity [12]

$$\int G(\mathbf{x}, \mathbf{x}_1; \eta) G^{-1}(\mathbf{x}_1, \mathbf{x}_0; \eta) \mathrm{d}\mathbf{x}_1 = \delta(\mathbf{x} - \mathbf{x}_0). \tag{A5}$$

Varying equation (A5), we obtain

$$\frac{\delta G(\mathbf{x}, \mathbf{x}'; \eta)}{\delta \eta(\mathbf{x}'')} = \iint G(\mathbf{x}, \mathbf{x}_1; \eta)\Gamma(\mathbf{x}_1, \mathbf{x}_2; \eta; \mathbf{x}'') G(\mathbf{x}_2, \mathbf{x}'; \eta) d\mathbf{x}_1 d\mathbf{x}_2, \tag{A6}$$

where the following notation is introduced:

$$\Gamma(\mathbf{x}_1, \mathbf{x}_2; \eta; \mathbf{x}'') = -\delta G^{-1}(\mathbf{x}_1, \mathbf{x}_2; \eta)/\delta \eta(\mathbf{x}''). \tag{A7}$$

Substituting equation (A6) into equation (A3) and equation (A3) into equation (A2), we obtain

$$\begin{aligned} G(\mathbf{x}, \mathbf{x}_0; \eta) = g(\mathbf{x}, \mathbf{x}_0) + \int G(\mathbf{x}, \mathbf{x}'; \eta)\eta(\mathbf{x}') g(\mathbf{x}', \mathbf{x}_0) d\mathbf{x}' + \gamma^2 \iiiint K(\mathbf{x}', \mathbf{x}'') \\ \times G(\mathbf{x}, \mathbf{x}_1; \eta)\Gamma(\mathbf{x}_1, \mathbf{x}_2; \eta; \mathbf{x}'') G(\mathbf{x}_2, \mathbf{x}'; \eta) g(\mathbf{x}', \mathbf{x}_0) d\mathbf{x}' d\mathbf{x}'' d\mathbf{x}_1 d\mathbf{x}_2, \end{aligned} \tag{A8}$$

Next cumbersome operations with equation (A8) are carried out, which we describe here briefly. We divide equation (A8) by $G(\tilde{\mathbf{x}}, \mathbf{x}; \eta)$ and integrate it in $\mathbf{x}$. According to equation (A5) the left-hand side of this equation turns into the Dirac delta function $\delta(\mathbf{x}_0 - \tilde{\mathbf{x}})$. The two corresponding $\delta-$functions are also formed on the right-hand side of the equation. We divide the resulting equation by $g(\mathbf{x}_0, \tilde{\tilde{\mathbf{x}}})$ and integrate over $\mathbf{x}_0$. Upon integrating over all $\delta-$functions and transferring the first term of the equation from the right-hand side to the left-hand side, we obtain

$$\begin{aligned} g^{-1}(\tilde{\mathbf{x}}, \tilde{\tilde{\mathbf{x}}}) - G^{-1}(\tilde{\mathbf{x}}, \tilde{\tilde{\mathbf{x}}}; \eta) = \eta(\tilde{\mathbf{x}})\delta(\tilde{\mathbf{x}} - \tilde{\tilde{\mathbf{x}}}) + \gamma^2 \int\int K(\tilde{\tilde{\mathbf{x}}}, \mathbf{x}'')\Gamma(\tilde{\mathbf{x}}, \mathbf{x}_2; \eta; \mathbf{x}'') G(\mathbf{x}_2, \tilde{\tilde{\mathbf{x}}}; \eta) \\ \times d\mathbf{x}'' d\mathbf{x}_2. \end{aligned} \tag{A9}$$

We vary equation (A9) with respect to η and use equation (A5) and the formula [12, 13]

$$\delta\eta(\tilde{\mathbf{x}})/\delta\eta(\mathbf{x}_3) = \delta(\tilde{\mathbf{x}} - \mathbf{x}_3). \tag{A10}$$

The first term in equation (A9) vanishes, and we obtain the general form of the equation that generates series expansion of the vertex function:

$$\begin{aligned} \Gamma(\tilde{\mathbf{x}}, \tilde{\tilde{\mathbf{x}}}; \eta; \mathbf{x}_3) = \delta(\tilde{\mathbf{x}} - \mathbf{x}_3)\delta(\tilde{\mathbf{x}} - \tilde{\tilde{\mathbf{x}}}) + \gamma^2 \iiint\int K(\tilde{\tilde{\mathbf{x}}}, \mathbf{x}'')\Gamma(\tilde{\mathbf{x}}, \mathbf{x}_2; \eta; \mathbf{x}'') G(\mathbf{x}_2, \mathbf{x}_4; \eta) \\ \times \Gamma(\mathbf{x}_4, \mathbf{x}_5; \eta; \mathbf{x}_3) G(\mathbf{x}_5, \tilde{\tilde{\mathbf{x}}}; \eta) \mathrm{d}\mathbf{x}'' \mathrm{d}\mathbf{x}_2 \mathrm{d}\mathbf{x}_4 \mathrm{d}\mathbf{x}_5 + \gamma^2 \iint K(\tilde{\tilde{\mathbf{x}}}, \mathbf{x}'') \\ \times G(\mathbf{x}_2, \tilde{\tilde{\mathbf{x}}}; \eta)\delta\Gamma(\tilde{\mathbf{x}}, \mathbf{x}_2; \eta; \mathbf{x}'')/\delta\eta(\mathbf{x}_3) \mathrm{d}\mathbf{x}'' \mathrm{d}\mathbf{x}_2. \end{aligned} \tag{A11}$$

Writing equation (A8) for $\eta = 0$ and introducing an appropriate designation for the self-energy Σ, we obtain two exact equation: the Dyson equation and the equation of connection Σ

with Γ. Restricting ourselves to the second term on the right-hand side of equation (A11), we obtain at $\eta = 0$ an approximate equation for Γ.

References

[1] Migdal A B 1958 *Zh. Eksp. Teor. Fiz.* **34** 1438
Migdal A B 1958 *Sov. Phys. JETP* **7** 996
[2] Eliashberg G M 1960 *Zh. Eksp. Teor. Fiz.* **38** 966
Eliashberg G M 1960 *Sov. Phys. JETP* **11** 696
[3] Pines D 1961 *The Many-Body Problem* (New York: Benjamin)
Pines D 1963 *Problema Mnogih Tel.* ed I A Kvasnikova (Moscow: Izdatel'stvo inostrannoj literatury)
[4] Pines D 1963 *Polarons and Excitons* ed C G Kuper and G D Whitfield (New York: Plenum)
[5] Puff R and Whitfield G 1963 *Polarons and Excitons* ed C G Kuper and G D Whitfield (New York: Plenum)
[6] Kraichnan R H 1961 *J. Math. Phys.* **2** 124
[7] Bruus H and Flensberg K 2002 *Introduction to Many-Body Quantum Theory in Condensed Matter Physics* (Copenhagen: Orsted Laboratory, Niels Bohr Institute)
[8] Sadovskii M V 2005 *Diagrammatika. Lektsii po izbrannym zadacham teorii kondensirovannogo sostoyaniya (Izdaniye vtoroye)* (Yekaterinburg: Institut elektrofiziki UrO RAN)
Sadovskii M V 2006 *Diagrammatics: Lectures on Selected Problems in Condensed Matter Theory* (Singapore: World Scientific)
[9] Bogolyubov N N and Shirkov D V 1957 *Vvedeniye v teoriyu kvantovykh poley* (Moscow: Fizmatlit)
Bogoliubov N N and Shirkov D V 1959 *Introduction to the Theory of Quantized Fields* (New York: Interscience)
[10] Engelsberg S and Schrieffer J R 1963 *Phys. Rev.* **131** 993
[11] Abrikosov A A, Gorkov L P and Dzyaloshinski I E 1962 *Metody kvantovoy teorii polya v statisticheskoy fizike* (Moscow: Fizmatgiz)
Abrikosov A A, Gorkov L P and Dzyaloshinski I E 1963 *Methods of Quantum Field Theory in Statistical Physics* (Englewood Cliffs: Prentice-Hall)
[12] Tatarskii V I 1967 *Rasprostraneniye voln v turbulentnoy atmosfere* (Moscow: Nauka)
Tatarskii V I 1967 *Wave Propagation in a Turbulent Medium* (New York: Dover)
[13] Klyatskin V I 2008 *Stokhasticheskiye uravneniya (Tom 1)* (Moscow: Fizmatlit)
Klyatskin V I 2005 *Stochastic Equations through the Eye of the Physicist (Vol.1.)* (Amsterdam: Elsevier)
[14] Armad N A and Sekistov V N 1980 *Izv. Vuzov Radiofizika* **23** 555
[15] Zernov N N 1982 *Izv. Vuzov Radiofizika* **25** 520
[16] Sekistov V N 1983 *Radiotekh. Elektron.* **7** 1262
[17] Ignatchenko V A and Polukhin D S 2013 *Zh. Eksp. Teor. Fiz.* **143** 238
Ignatchenko V A and Polukhin D S 2013 *JETP* **116** 206
[18] Ignatchenko V A and Polukhin D S 2013 *Zh. Eksp. Teor. Fiz.* **144** 972
Ignatchenko V A and Polukhin D S 2013 *JETP* **117** 846
[19] Cai J, Lei X L and Xie L M 1989 *Phys. Rev.* B **39** 11618
[20] Kostur V N and Mitrovic B 1994 *Phys. Rev.* B **50** 12774
[21] Grimaldi C, Pietronero L and Strassler S 1995 *Phys. Rev. Lett.* **75** 1158
[22] Takada Y and Higuchi T 1995 *Phys. Rev.* B **52** 12720
[23] Danylenko O V, Dolgov O V and Losyakov V V 1997 *Phys. Lett.* A **230** 79
[24] Ummarino G A and Gonnelli R S 1997 *Phys. Rev.* B **56** R14279
[25] Cosenza F, De Cesare L and Fusco Girard M 1999 *Phys. Rev.* B **59** 3349
[26] Danylenko O V and Dolgov O V 2001 *Phys. Rev.* B **63** 094506
[27] Hague J P and d'Ambrumenil N 2008 *J. Low Temp. Phys.* **151** 1149
[28] Johannes B, Jong E H and Olle G 2011 *Phys. Rev.* B **84** 184531
[29] Bourret R C 1962 *Nuovo Cimento* **26** 1
[30] Rytov S M, Kravtsov Y A and Tatarskii V I 1978 *Vvedenie v Staticheskuju Radiofiziku (Chast' II: Sluchajnye Polja)* (Moscow: Nauka)

Rytov S M, Kravtsov Y A and Tatarskii V I 1988 *Principles of Statistical Radiophysics (Volume 2: Correlation Theory of Random Processes)* (Berlin: Springer)
[31] Lado S K 2007 *Lektsii o proizvodyashchikh funktsiyakh* (Moscow: MTSNMO)
[32] Furutsu K 1963 *J. Res. NIST* **67D** 303
[33] Novikov E A 1964 *Zh. Eksp. Teor. Fiz.* **47** 1919
Novikov E A 1965 *Sov. Phys. JETP* **20** 1290